PNNL-17498

Pacific Northwest National Laboratory
Operated by Battelle for the U.S. Department of Energy

Modeling Light Capture Efficiency on Various Radiation Detector Geometries Using Monte-Carlo Optical Transport Software

Sean E. Jones[(1)],
Justin I. McIntyre[(2)],
Matthew W. Cooper[(2)],
Marty E. Keillor[(2)],
Scott D. Kiff[(2)],
Hui Tan[(3)]

1) Department of Nuclear Engineering and Radiation Health Physics, Oregon State University, Corvallis, Oregon, 97331

2) Pacific Northwest National Laboratory, P.O. Box 999, Battelle Blvd, Richland WA 99353

3) XIA LLC, 31057 Genstar Rd. Hayward CA 94544

December 2007

Prepared for the U.S. Department of Energy
under Contract DE-AC06-76RL01830

PACIFIC NORTHWEST NATIONAL LABORATORY
operated by
BATTELLE
for the
UNITED STATES DEPARTMENT OF ENERGY
under Contract DE-AC05-76RL01830

Printed in the United States of America

Available to DOE and DOE contractors from the
Office of Scientific and Technical Information,
P.O. Box 62, Oak Ridge, TN 37831-0062;
ph: (865) 576-8401
fax: (865) 576-5728
email: reports@adonis.osti.gov

Available to the public from the National Technical Information Service,
U.S. Department of Commerce, 5285 Port Royal Rd., Springfield, VA 22161
ph: (800) 553-6847
fax: (703) 605-6900
email: orders@ntis.fedworld.gov
online ordering: http://www.ntis.gov/ordering.htm

This document was printed on recycled paper.
(9/2003)

PNNL-17498

Modeling Light Capture Efficiency on Various Radiation Detector Geometries Using Monte-Carlo Optical Transport Software

Sean E. Jones(1),
Justin I. McIntyre(2),
Matthew W. Cooper(2),
Marty E. Keillor(2),
Scott D. Kiff(2),
Hui Tan(3)

1) Department of Nuclear Engineering and Radiation Health Physics, Oregon State University, Corvallis, Oregon, 97331

2) Pacific Northwest National Laboratory, P.O. Box 999, Battelle Blvd, Richland WA 99353

3) XIA LLC, 31057 Genstar Rd. Hayward CA 94544 December 2007

Prepared for the U.S. Department of Energy
under Contract DE-AC06-76RL01830

Pacific Northwest National Laboratory
Richland, Washington 99352

Executive Summary

This paper investigates the optimization of light capture efficiency in a two scintillation cell radiation detector. Using computational Monte-Carlo transport methods to model the generation and ultimate capture efficiency of optical photons it was possible to compare several different optical geometries. This capture efficiency is a critical factor in the quality of the overall energy resolution and detection efficiency of scintillation detectors. The results of this study have been applied to a new beta-gamma detector designed to monitor atmospheric levels of radioxenon. The results of this study can also be applied to the design considerations of future scintillation based radiation detection methods.

Objectives:

The primary objective of this research is to determine geometric considerations for optimal light capture efficiency in the beta cell of a coincidence beta-gamma detector that consists of two different scintillators, (Cooper et al, 2007). This research is applicable to the improvement of the performance of all scintillation based radiation detection systems. The energy resolution and detection efficiency are a direct outcome of the scintillation photon capture efficiency within the photo-multiplier-tube (PMT). The secondary objective of this research is to develop a general and qualitative understanding of the effects on light capture efficiency of geometric and reflective properties in scintillation based radiation detectors. This objective was accomplished by the investigation and comparison of eight different optical geometries. Qualitative and quantitative understanding of these results can than be applied to improve the development and production of other scintillation based radiation detection systems.

Background:

This report is a contribution to the development of a beta-gamma radiation detector specialized for the monitoring of atmospheric levels of radioxenon as called for by the Comprehensive-Test-Ban-Treaty-Organization (Prep. Com., 1999). This research is conducted as a part of a Graduate Research Internship at Pacific Northwest National Laboratory, run by the Battelle Memorial Institute for the United States Department of Energy.

Two schematic diagrams (Figure 1A and 1B) show the beta-gamma detector used to detect the four radioxenon isotopes ^{131m}Xe, 133mXe, ^{133}Xe and ^{135}Xe. The CsI(Na) well detectors are used to detect both x-rays and gamma-rays from the beta-gamma coincidence signatures of the four radioxenon isotopes. The plastic scintillator cell is used to detect beta particles and conversion electrons. The use of a single PMT for each detector greatly increases the detector calibration and reliability. However, it is critical to achieve good energy resolution with the beta cell to distinguish between overlapping signatures for ^{131m}Xe, ^{133m}Xe and ^{133}Xe, hence and important outcome of this research.

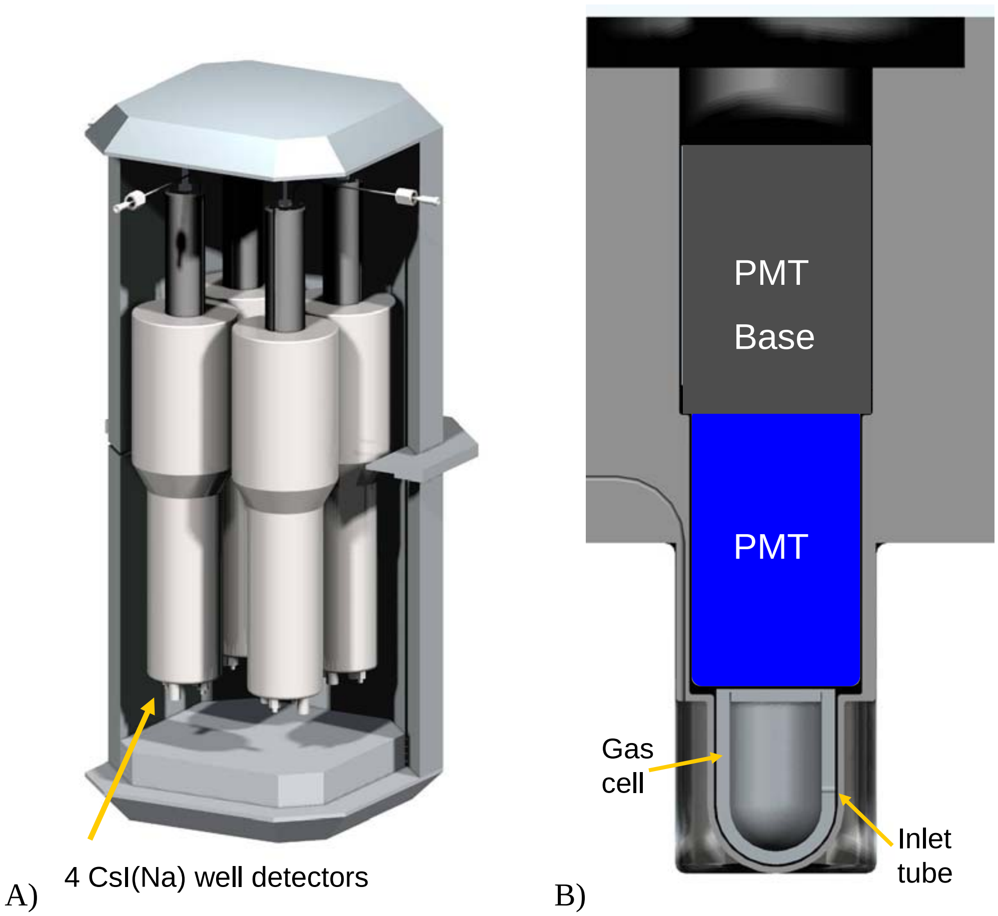

Figure 1A. Schematic of four CsI(Na) well detectors with gas beta cells, inside of 1" lead cave. The second schematic is the gas beta cell with PMT and tube base.

The Monte-Carlo software used in this study is known as DETECT2000. It was written by François Cayouette, as a portion of his Doctoral research at Laval University, Canada (Cayouette, 2001). DETECT2000 is a C++ programming language update of the DETECT97 software, which was based on the DETECT code. DETECT was originally written by Glenn Knoll in 1988 (Knoll et al., 1988). It was written in the Pascal programming language and was first used to investigate the optical performance properties of various potential designs for a scintillation based neutron detector.

Light capture efficiency in scintillation based radiation detection systems is of significance because optical capture is the mechanism that ultimately dictates the information gathered about radiation events occurring in the detector. This study considers optical photons captured when they strike the surface of the photomultiplier tube. In a real scintillation based radiation detection system, this event will result in an electronic signal that can be processed for information. As such, it can be said that light capture efficiency is important to this electronic signal for two reasons.

The first reason is signal to noise Ratio (SNR) which is inherent in any electronic system. The greater the signal strength over that noise, the smaller the contribution from the noise is to the system's output. This directly effect the detection efficiency of low level signals which can be obscured by the random noise fluctuations. The second reason is energy resolution; in this study, it is the comparison of an energy deposition in one part of the detector to the exact same event in another portion of the detector. The ability of these events to look the same in the diction system's output is dictated by the uniformity of light capture in the scintillator.

Method:

The results of this study were obtained by utilizing the DETECT2000 Monte-Carlo optical transport code. Due to the original source code's lack of compliance with current C++ computing language standards, ISO version 4.X, the binaries had to be built using a legacy C++ compiler, ISO version 2.9. The simulations of the radiation detector geometries were constructed as per technical drawings of the detector produced by the manufacturer, St. Gobain.

As the simulation relied on Monte-Carlo methods, certain optical properties of the material had to be defined. The optical properties of these materials are empirical and some of that data was not available so three of the properties were assumed. Table 1 lists out the values for each of the materials that were used in the simulations.

Material	Index of Refraction	Absorption Length (mm)	Wavelength of Emission (nm)
BC400 (Beta Cell)	1.58	1600	423
NaI	1.55	2500*	No Scintillations Simulated
Air	1.01	2500*	No Scintillations Simulated
PMT Photocathode, DETECT Surface	1.50	Not Applicable	Not Applicable

Table 1. Optical properties used in the simulations. Note (*) indicates property assumption.

It should be noted, that this simulation method was performed with a single wavelength of emission from the BC400 scintillator of the beta cell. However, it is known that scintillators emit light distributed throughout the optical spectrum. Although that data was available for BC400; without knowing the other optical properties, index of refraction and absorption length, for all of the photons in the spectrum, this would further complicate the results. It was decided to simulate the peak wavelength and use the known optical properties for the peak wavelength of emission. The effects of these assumptions are not known, however, these variances from real world physics properties are not considered to significantly alter the results.

A bug in the original software for specific geometric constructions allowed photons that did not escape the geometry to be counted as escaped. This was always a problem when the geometry had cylindrical volumes whose boundaries touched. This effect was termed the “False Escape Problem” by Hui Tan of X-ray Instrumentation Associates, (XIA) LLC. In an attempt to solve this issue, Tan added code to the original Photon.CPP source file. Using the new software algorithms, it was discovered that the results of undefined regions were treated optically as vacuum volumes. These vacuum volumes had indexes of refraction and possibility of absorption through path lengths traveled similar to the air volumes used in the simulation. Consequently, outputs from both binaries were very similar showing little to no variation on their solutions.

This was significant to the results as the new binary always output a “Segmentation Fault” error when trying to run the more geometrically complex Phoswich simulations. As such, the old binary was run for the two Phoswich geometry simulations, resulting in false photon escapes of approximately 4.5% on each of the data points.

While it cannot be determined exactly what would happen to those falsely escaped photons, comparison of the results from simulations that ran on both binaries showed that approximately 95% of the escaped photons would have been captured. Therefore, it is believed that this added an additional uncertainty of approximately 0.5% to the Phoswich simulation data, for a grand total of approximately 1% uncertainty for each data point on those two data sets. These assumptions were considered to be conservative for the current work.

The data presented on each of the eight simulations represents the generation of optical photons at 180 infinitesimally small data points. Each data point represents 10^5 photons simulated, for a grand total of 18 million photons generated per geometry. In the program's statistical output, the number of photons simulated yielded uncertainties on all of the results to be less than 0.2%. Furthermore, each data point had a unique seed for the random number generator, each seed providing a period of 10^{18} random numbers, ensuring proper behavior of individual random events (Cayouette et al., 2001).

To achieve uniform characterization, the area distribution of data points was equal for the majority of the detector simulated. This value was approximately 5 data points per mm^2. This distribution was achieved by the development of code in C++ that output text to use in the simulation construction input. There was a variation in the arc cross section area in the beta cell's spherical tip. This was performed to better assess the effects of light capture efficiency in this region. The data point distribution in that area were calculated by using a formula to distribute points along the radii, at angles of 18 degrees. The innermost and outermost points of all regions are within 0.1 mm of the material boundaries, and the distribution of data points in between is spatially uniform. This resulted in a data point distribution of approximately 10 per mm^2 for that region. The distribution of the data points within the beta cell tip is illustrated in Figure 2.

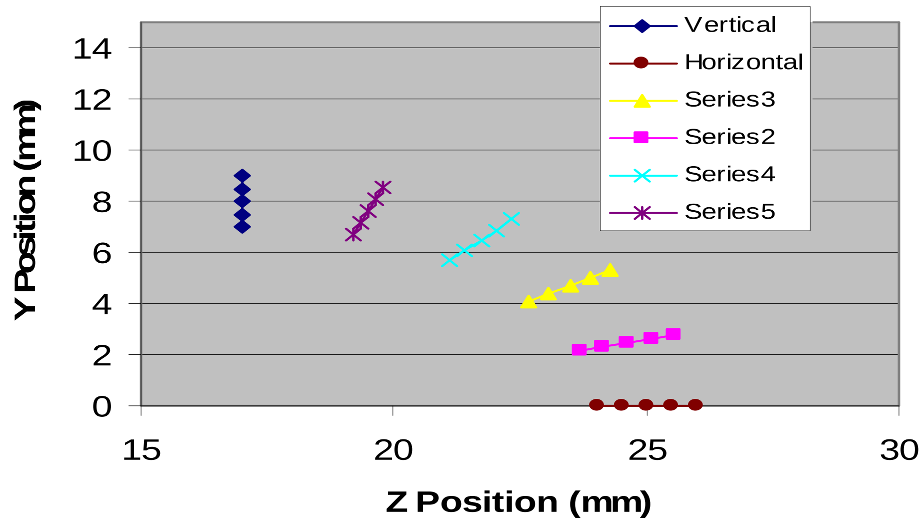

Figure 2. Position distribution of the simulation points in the spherical tip of the beta cell.

For the purposes of efficiency, the data points were placed on a plane in the scintillator about the lines of symmetry, as shown in Figure 4. This prevented unnecessary repetitive computations, and simplified the processes of compiling and presenting the data. Uniformity about the lines of symmetry was demonstrated in previous research using this software (Farsoni *et al.*, 2007).

In order to investigate the effects of certain changes on light capture efficiency, 4 designs were tested, each with different reflector placement. Each design was simulated twice, once using metalized reflectors and then again using diffuse reflectors; this resulted in a simulation total of 8 data sets, or 8 geometries. It should be noted that reflection probability was chosen as 95% at all reflective boundaries, as chosen in previous work in light capture efficiency, from data based on the CRC Handbook (Henning *et al.*, 2006).

As the program output data in large text files, custom software was written in the C++ programming language to parse through the output files to obtain and sort the desired data. For graphical representation, the data was input into Microsoft Excel and ROOT. Additional custom software was developed to quickly generate the code to produce the graphs in ROOT.

Due to the lack of graphical geometry output in DETECT2000, ROOT was used to represent the detector simulation construction in an interactive three-dimensional representation (****need ROOT reference). Screen shots of the results of this modeling are shown in Figures 3 through 5.

A) 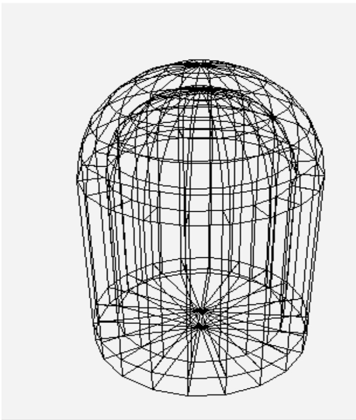 B) 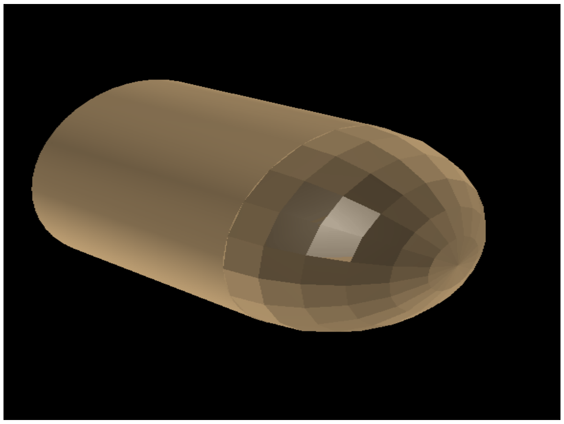

Figure 3A. wireframe representation of the simulated beta cell done using ROOT. Figure 3B. Exterior view of the simulated beta cell using ROOT.

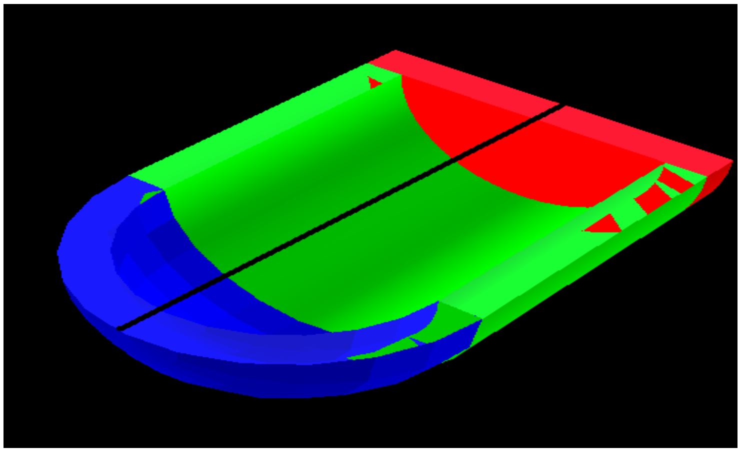

Figure 4. Graphic representation of the beta cell sliced through its 1st line of symmetry. The Black line superimposed on the graphic shows the 2nd line of symmetry along which the data points for the simulations were distributed about..

In all of the simulations, the data points in the beta cell were distributed in the scintillator area on the plane, about the 2nd line of symmetry, the black line bisecting the cell, as illustrated in Figure 4. For the purposes of optical photon detection, an invisible surface exists that counts all optical photons that strike it, its location is at the far end of the red colored base in this drawing. In the 1, 1.5, and 2 reflector geometries, this was all that was simulated as optical photons would not leave the beta cell.

The single reflector geometry is a simulation where the reflecting boundary completely surrounds the beta cell, the interior void is simulated as air. The 2 reflector geometry is the same as the single but it has an additional reflector completely surrounding the interior air volume. The 1.5 reflector geometry is like the single reflector model but an additional reflector is located on the interior base of the beta cell (red in figure 4).

Figure 5 represents the two Phoswich simulations. The grey beta cell exists within the well of the yellow NaI cell. Invisible surfaces at the exterior of the beta cell base that also spans the gap in the well between the beta cell and the NaI, and at the base of the NaI cell are the boundaries that count photons that strike them. In these simulations the reflecting boundary completely surrounded the exterior of the NaI well detector. In the phoswich simulations, optical photons were allowed to pass from the beta cell into the NaI well detector. Because the well detector is used to detect x-rays and gamma-rays only no optical photons were generated in this region of the phoswich detector.

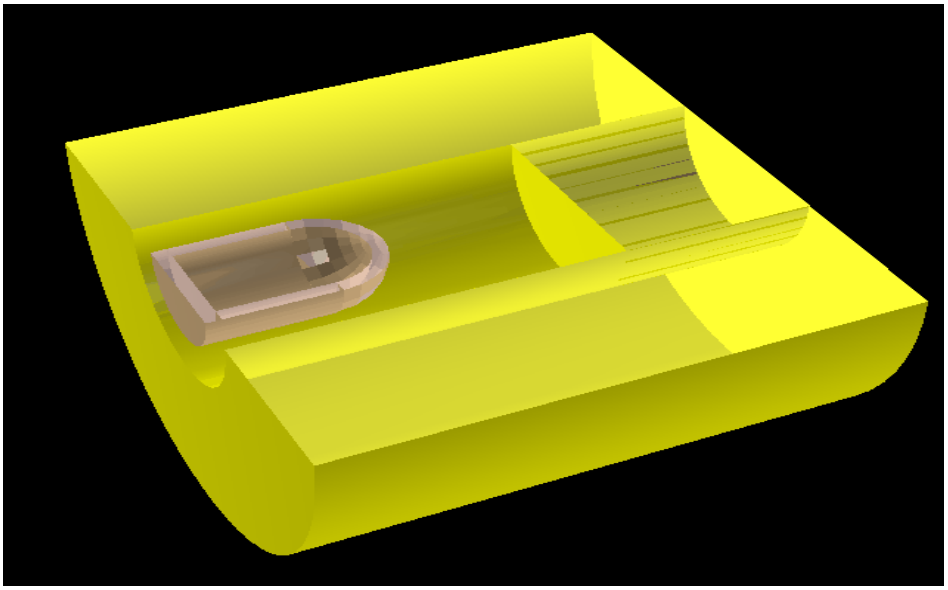

Figure 5. Graphic representation of a slice through the phoswich simulation about its 1st line of symmetry.

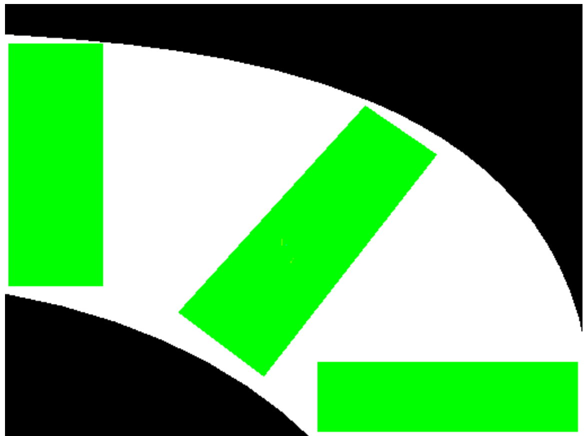

Figure 6. Graphical representation of the last 3 data set lines, as distributed in the arc cross-section of the beta cell tip.

Results:

The results for each of the simulations is shown using a pair of graphs that display the photon capture efficiency in two-dimensions and three-dimensions. Within the first graph the base of the beta cell is indicated in red (high efficiency) along the y-axis. The walls of the cells are represented along the top of the graph and as expected have falling efficiencies as the distance from the base. The tip is represented with a diagonal line in the upper most right hand corner.

For the purpose of understanding the beta cell tip data shown in this section, refer to figure 6. Each line represents five data points equally spaced, on the radii of the geometry, spanning the cross section, at 90, 54, and 0 degrees with respect to the horizontal. This placement is carried onto the last 3 lines in the graphical representations of the data that demonstrate light capture efficiency versus position within the detector. There are actually 6 lines of data in the beta cell tip, however, for the purposes of visual clarity, 3 lines were omitted from the graphical representations of the data. The actual distribution on the data points in the tip is shown in Figure 2.

Figures 7 through 10 demonstrate the effects of a diffuse reflector used in the design. These data sets show that in the 1 and 2 reflector designs, a diffuse reflector will lead to a smooth transition of decreasing light capture efficiency as light is generated further from the Photomultiplier Tube (PMT). Possibly, this effect occurs due to the random scattering angle at each successful reflection, with each potential reflection yielding a 5% chance of photon death. Consequently, the further away a photon is generated, the more reflections a photon is likely to encounter, the higher its chance of death, the less its probability of capture is. This hypothesis is further substantiated when comparing Figures 7 and 8 to Figures 9 and 10; as the 2 reflector geometry has a greater surface area for reflection, thus leading to more light reflections in the thin and remote portions of its volume than the 1 reflector geometry; hence the increase in observation of this effect when comparing 1 diffuse reflector to 2 diffuse reflectors.

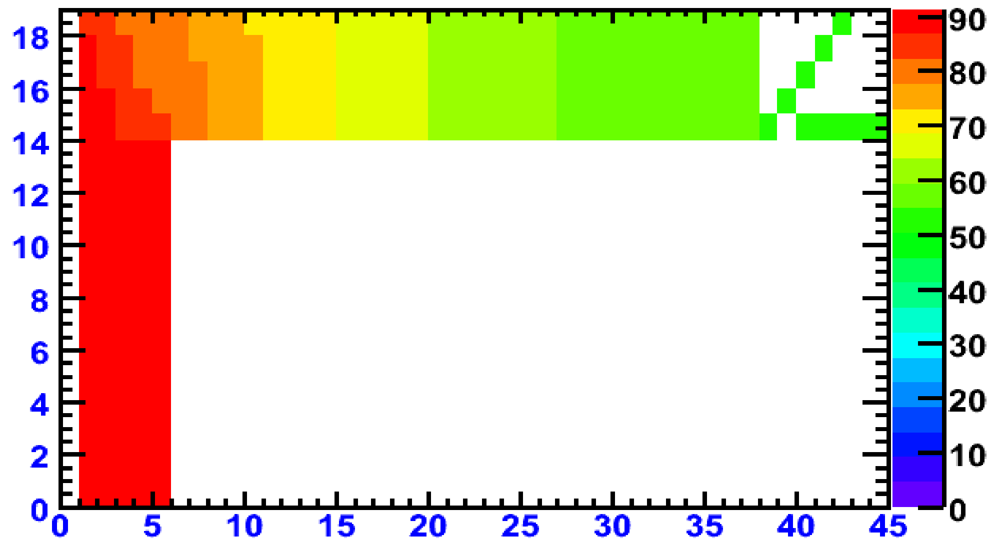
18
16
14
12
10
8
6
4
2
0
0
5
10
15
20
25
30
35
40
45
90
80
70
60
50
40
30
20
10
0

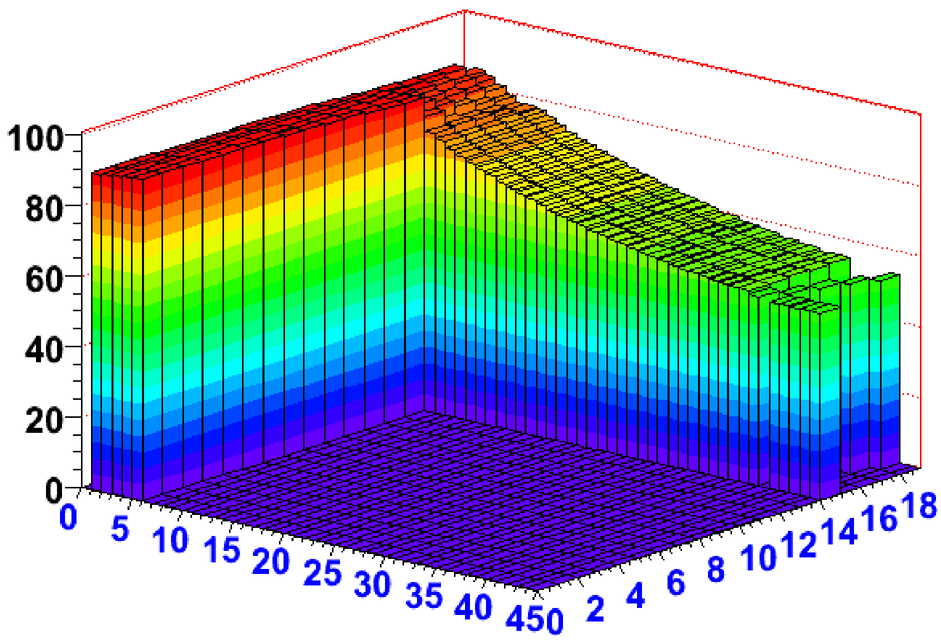
100
80
60
40
20
0
0
5
10
15
20
25
30
35
40
45
0
2
4
6
8
10
12
14
16
18

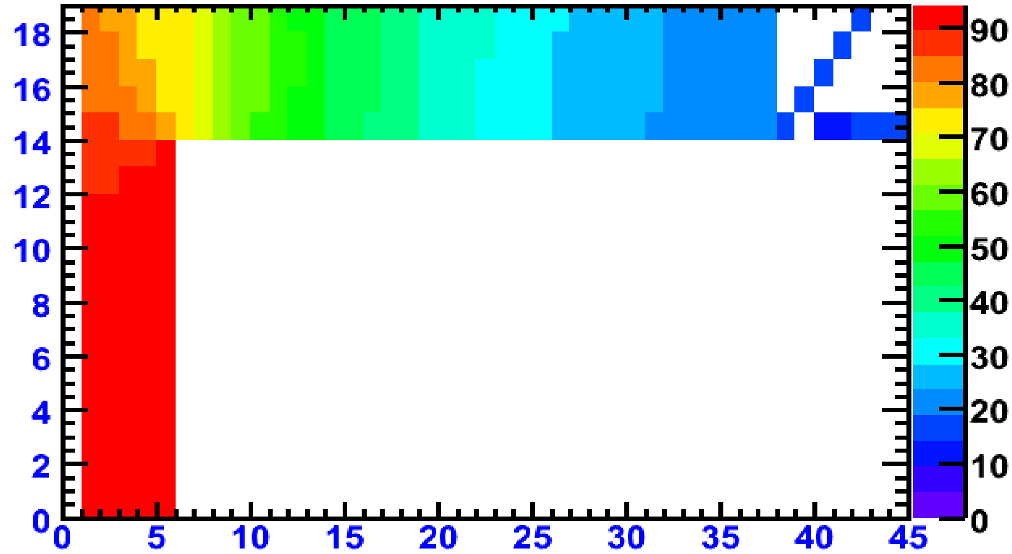

Figure 9, T
with 2 diff

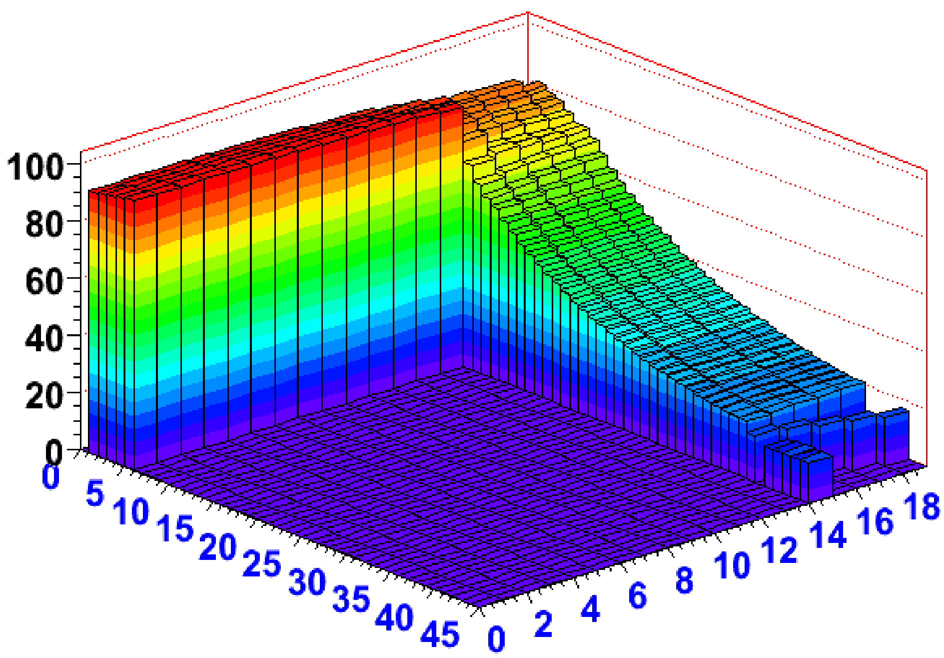

in the beta
cell with 2 diffuse reflectors.

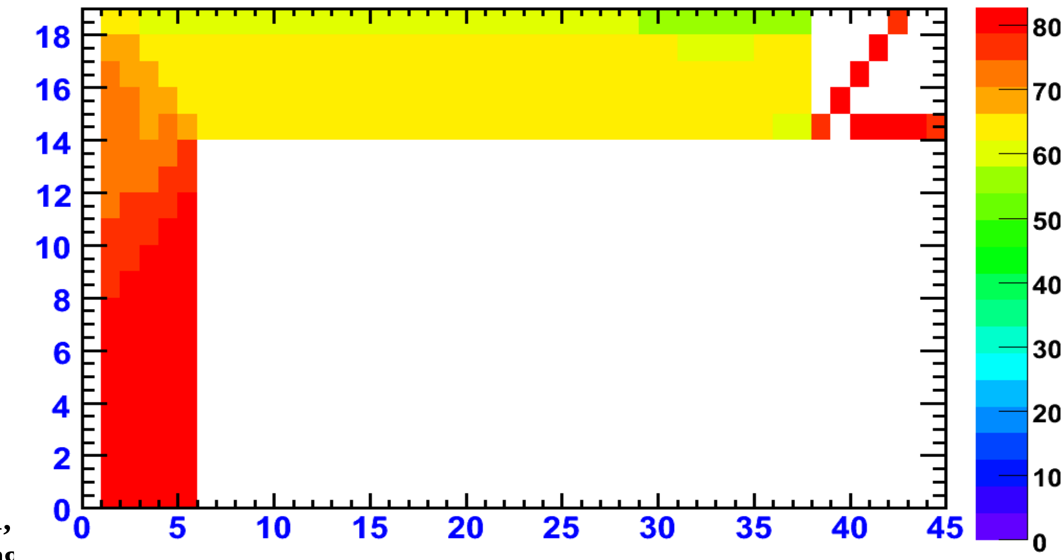

Figure 11,
with a sing

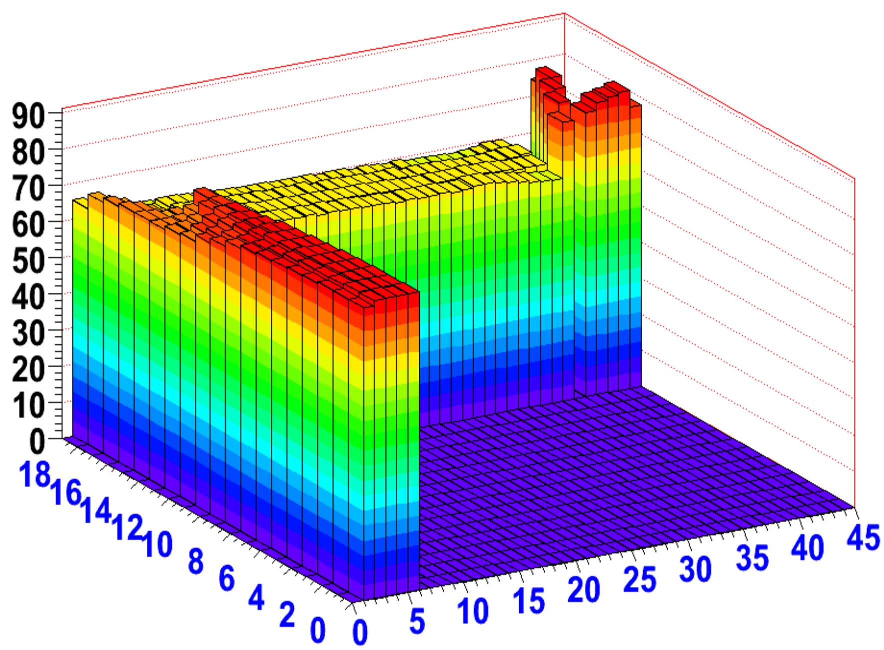

Figure 12.
cell with a

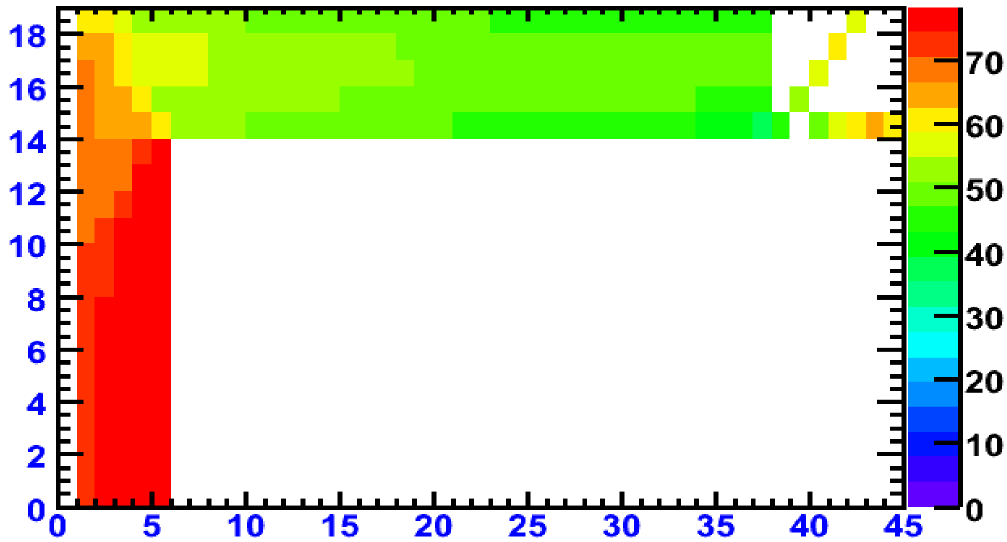

Figure 13,
with 2 met

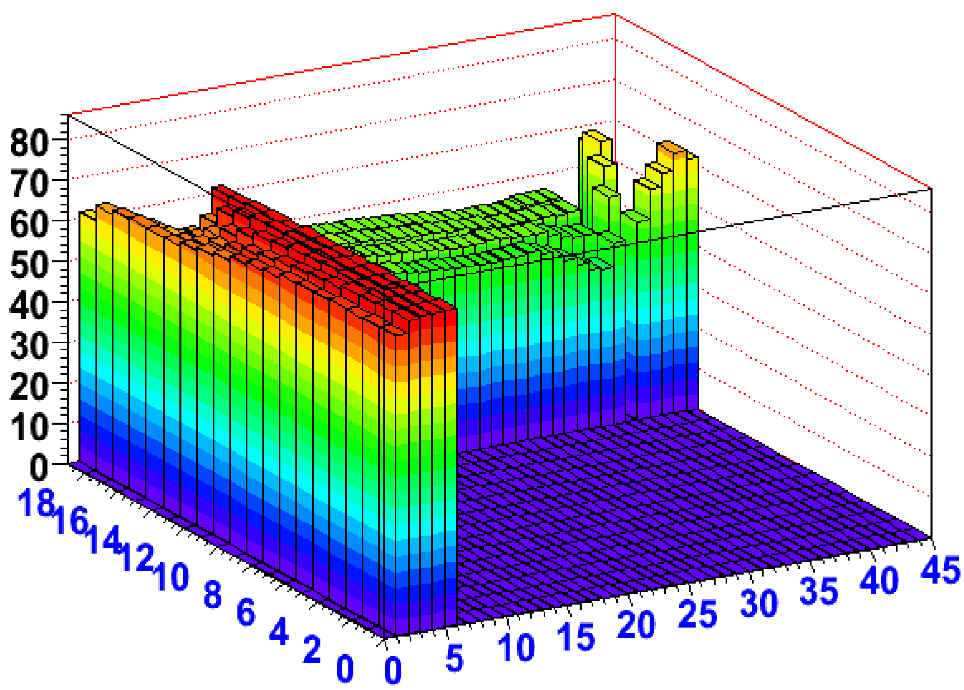

Figure 14 '
cell with 2

Figures 11 through 14 demonstrate the effects of a metallized reflector used in the design. These data sets show that in our 1 and 2 reflector designs, a metal reflector does not yield a smooth transition of decreasing light capture efficiency as light is generated further from the PMT. Furthermore, the heightened light capture efficiency in the last 2 data lines, the ones deep in the beta cell tip, show a marked and rapid increase in light capture efficiency in that region; in particular, that it is at a local maximum at the most remote location, the data taken on the line of symmetry in the beta cell tip. It is believed that this effect is observed due to the reflective properties a metallized surface provides. At the line of symmetry, in the most remote region, the light generated will be reflected in directions that can only lead closer towards successful capture. Conversely, as light is generated further from this region, some of that light can still travel away from successful capture, resulting in a smaller chance of optical capture due to greater travel length as well as a greater probability of reflections. A comparison between the data sets of Figures 11 and 12 to Figures 13 and 14, show the effects of decreased light capture efficiency as the surface area of reflective boundaries is increased as apparent in the comparison of Figures 7 and 8 to Figures 9 and 10.

Figure 15 illustrates the probability distribution of light capture efficiency for all 1 and 2 reflector geometries. In general, this figure demonstrates the advantages of metallized versus diffuse reflectors used in our closed beta cell geometry, as the metallized reflectors show a less broad spectrum of light capture efficiencies and an overall increase in light capture efficiency.

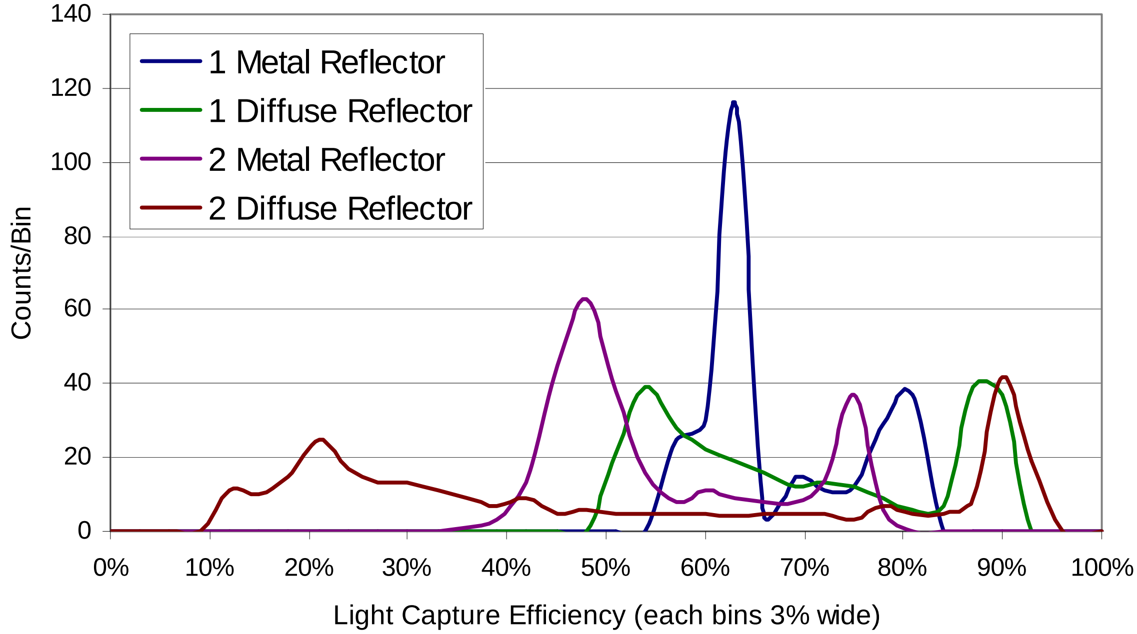

Figure 15. Probability Distribution of Light Capture Efficiency in the Beta Cell, 1 and 2 Reflector Geometries.

Figures 16 through 19 illustrate the positional dependence of light capture efficiency for the 1.5 reflector geometries. These two data sets show the same trend of positional dependence of light capture efficiency when comparing metallized to diffuse reflector geometries, as discussed in Figures 7 through 14. However, as seen in Figure 25, their overall light capture efficiencies are smaller by comparison to their 1 and 2 reflector geometry counterparts, with the exception of the 2 diffuse reflector geometry.

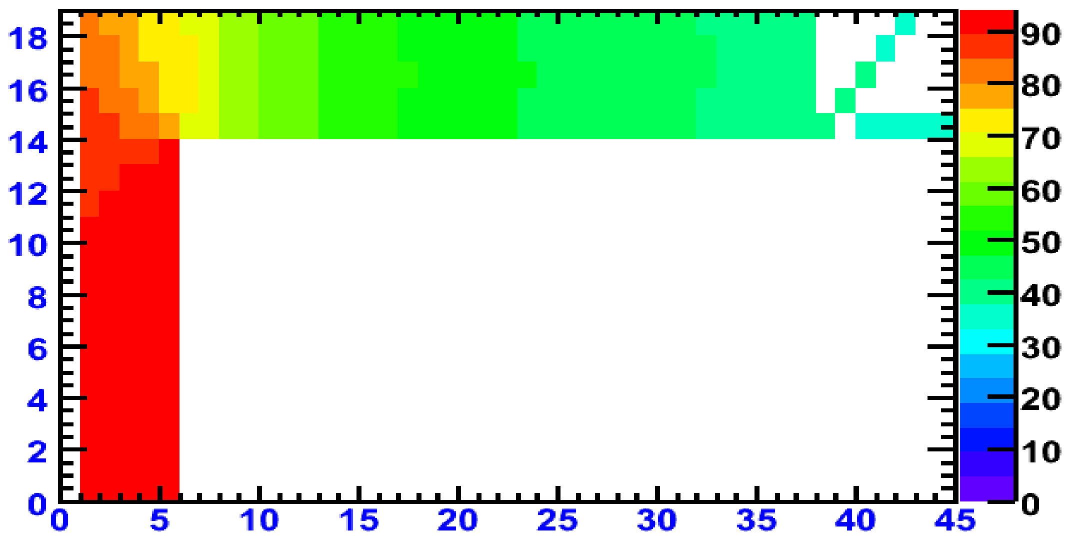

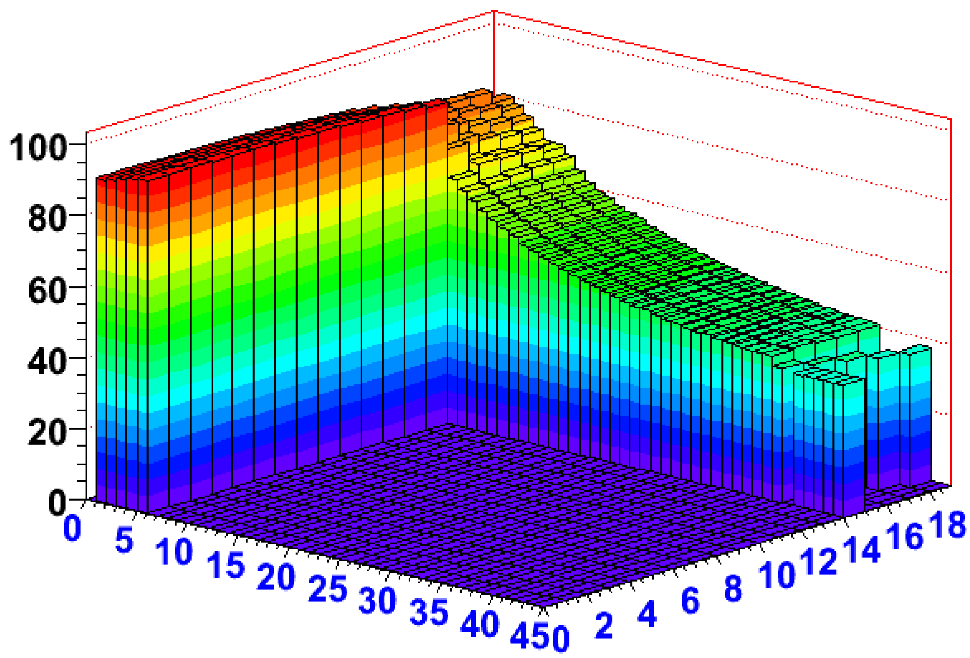

Figure 17.
Cell with 1

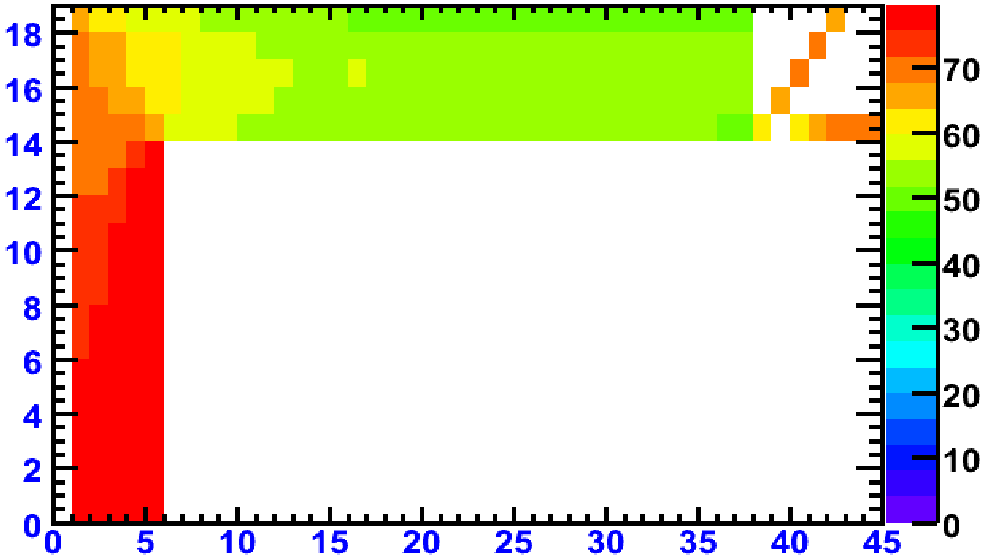

I e beta cell
with 1.5 metal reflectors.

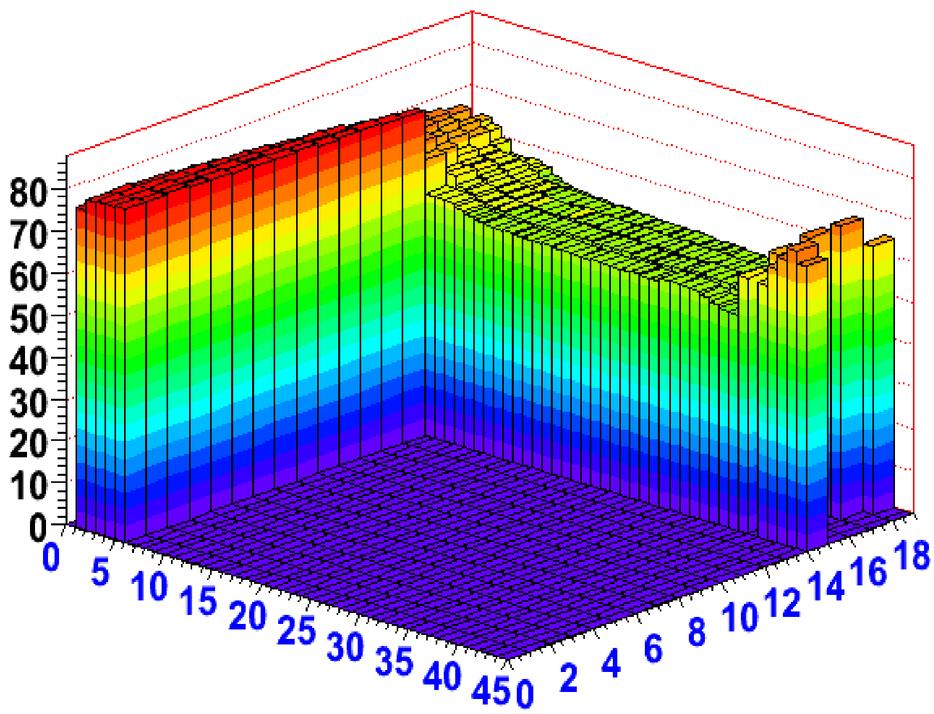

Figure 19.
cell with 1.

Figures 20 through 23 illustrate the positional dependence of light capture efficiency for the 2 PMT, Phoswich geometries. Since this geometry is now surrounded by a simple geometry of reflector, their data sets are very similar in appearance, and it is difficult to make a comparison of these two geometries using those figures. However, Figure 24 is more suited to make a comparison, showing the probability distribution of light capture efficiency comparison for these two geometries. This data representation clearly shows a slightly higher overall light capture efficiency and slightly less broad distribution for the diffuse reflector geometry.

Figures 25 through 27 represent the probability distributions of light capture efficiency for all of the geometries, with various amounts of data points. In general, when comparing Figure 25 to Figure 26, all of the data points to ½ of the data points, changes in the shapes of the distributions are not easily as apparent when comparing Figure 26 to Figure 27, ½ of the data points to ¼ of the data points. This trend suggests that enough data points have been distributed to adequately characterize the probability distribution of the geometries tested.

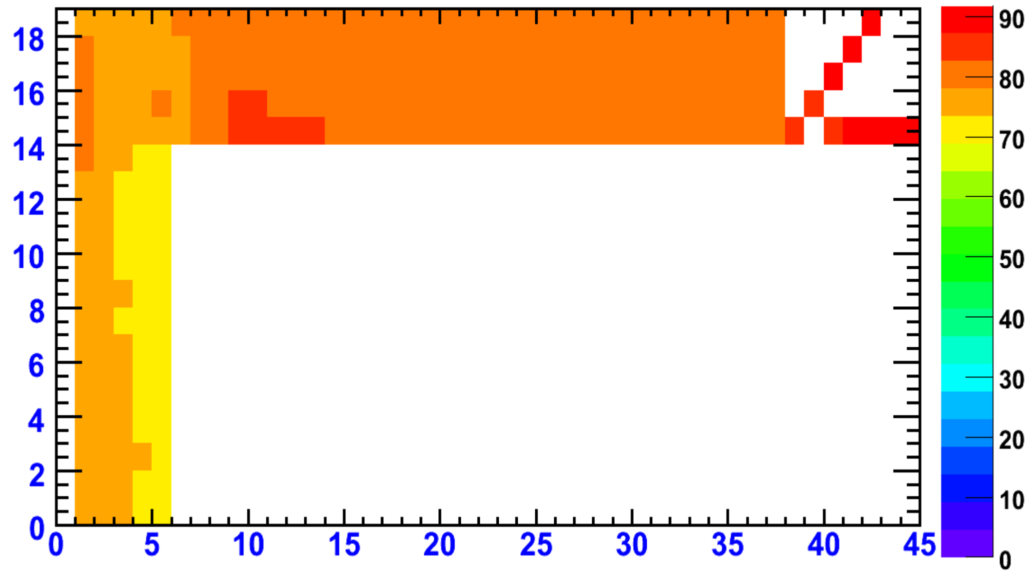

Figure 20.
phoswich l

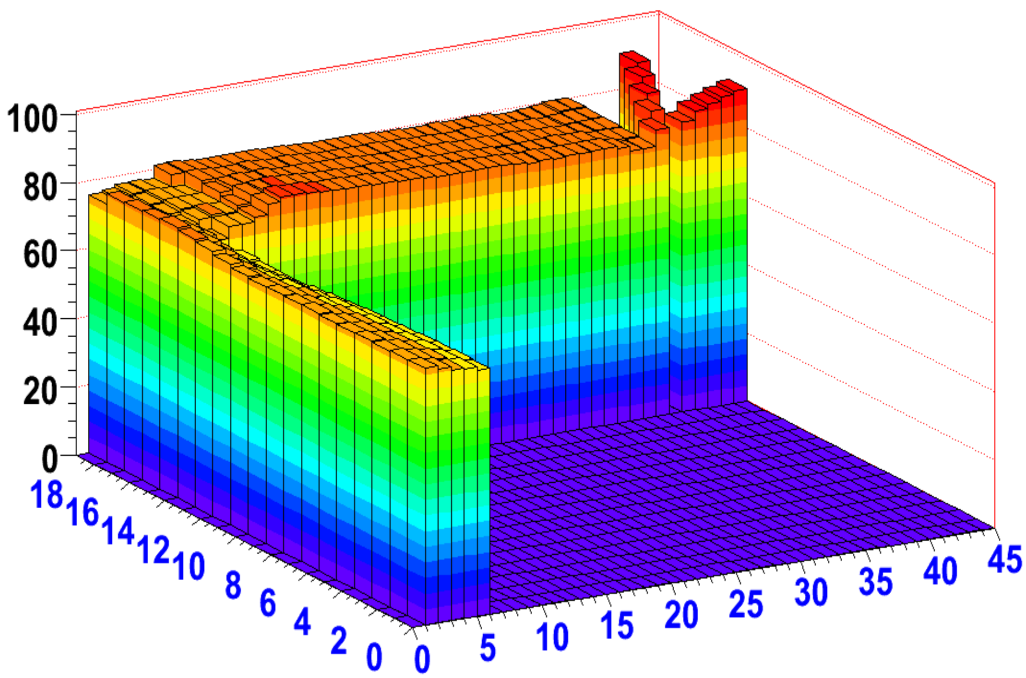

Figure 21.
phoswich l

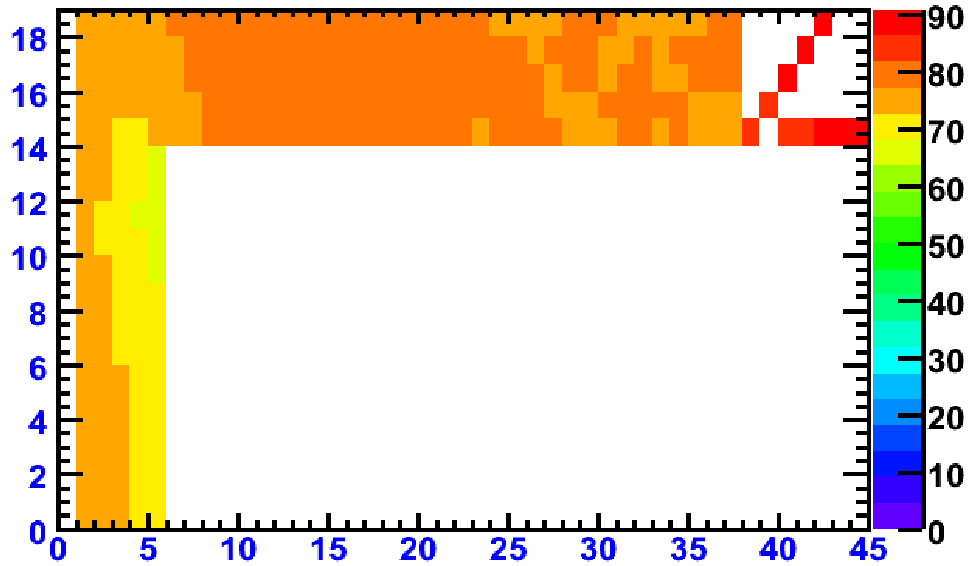

the
phoswich beta cell with metal reflector.

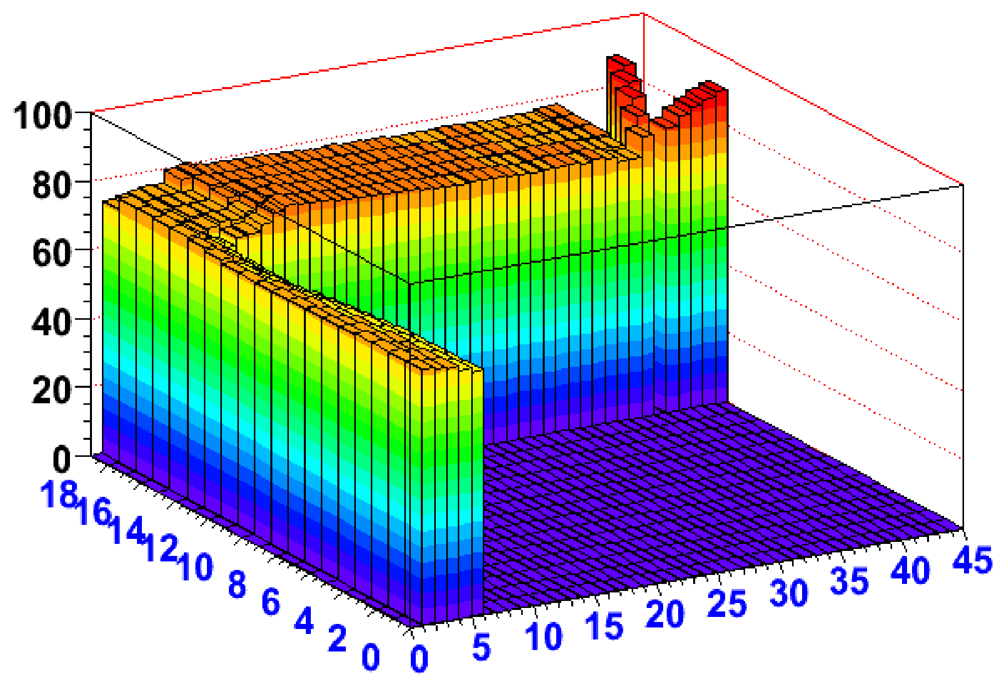

Figure 23.
phoswich l

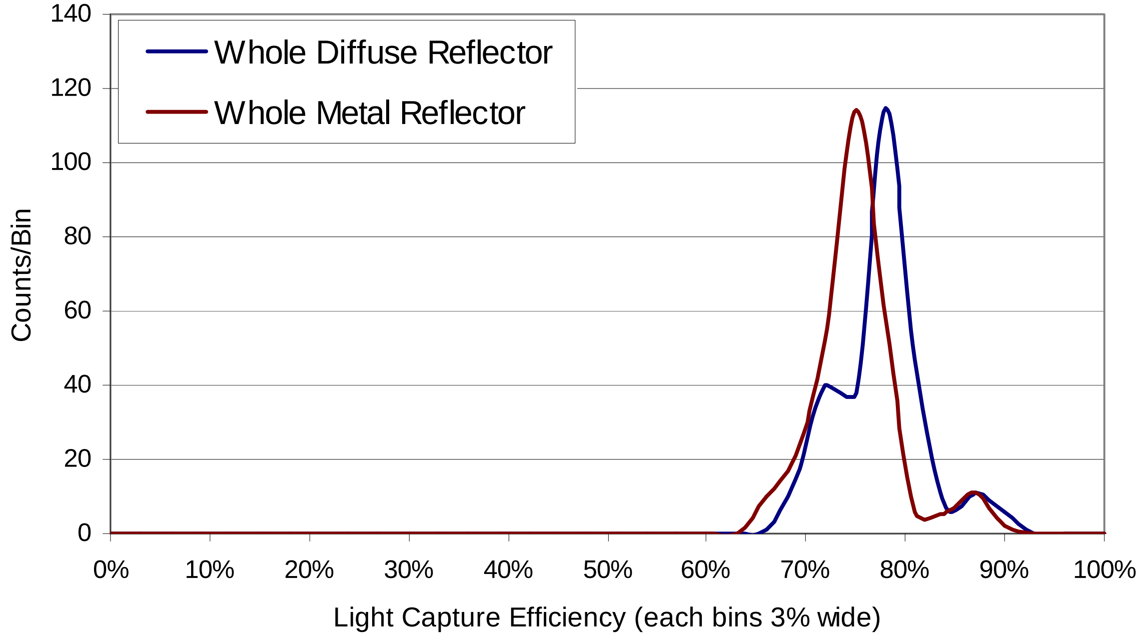

Figure 24. Probability distribution of light capture efficiency for all geometries.

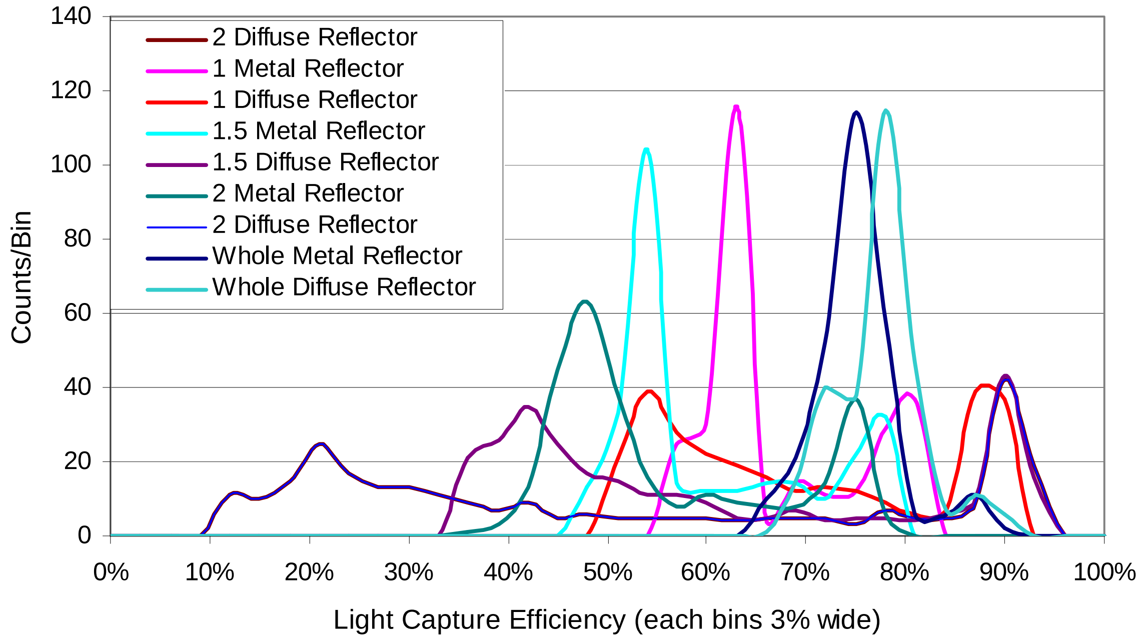

Figure 25. Probability distribution of light capture efficiency for all geometries.

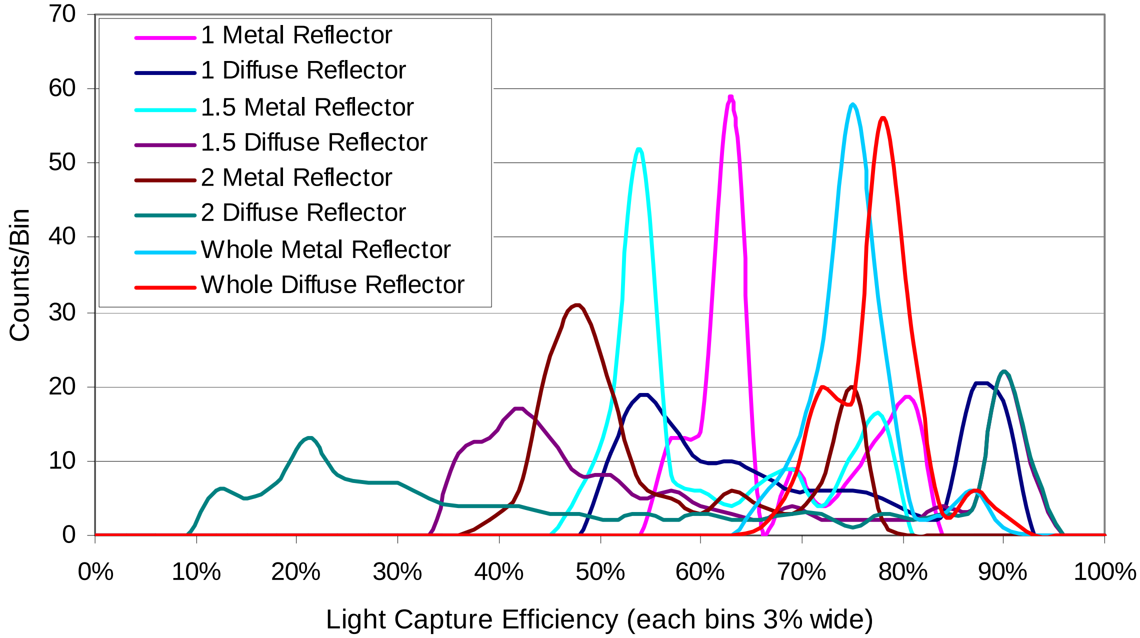

Figure 26. Probability distribution of light capture Efficiency for all geometries using half of the data points.

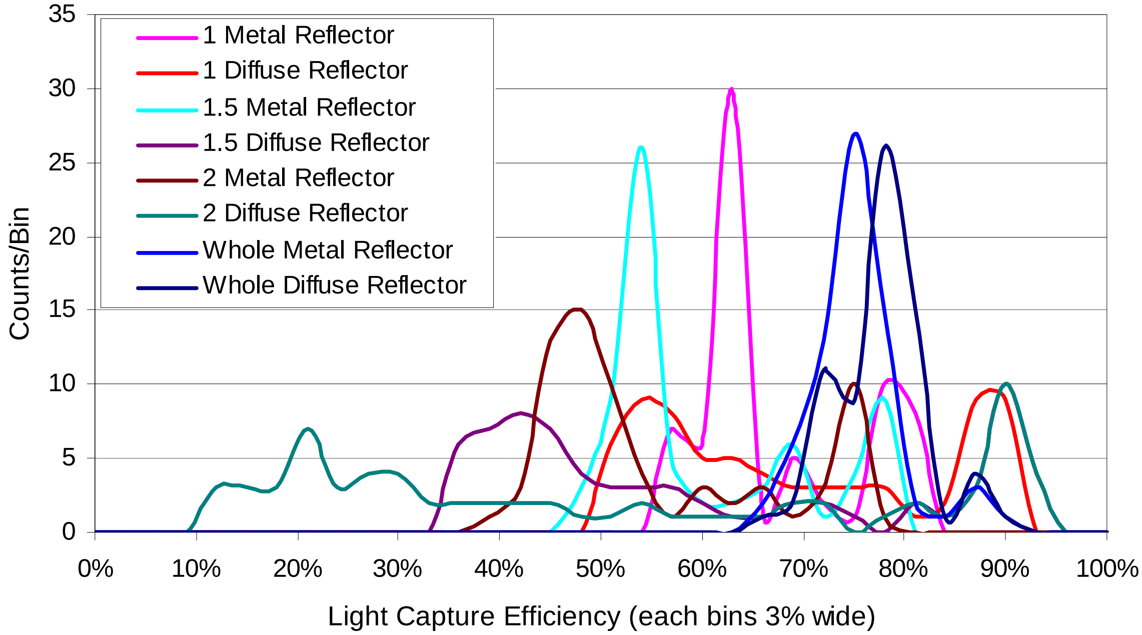

Figure 27. Probability distribution of light capture Efficiency for all geometries using one-quarter of the data points.

Conclusions and Future Work:

The results of this study suggest, that for the purposes of maximizing light capture efficiency and minimizing its distribution, the detector design modeled should use a Phoswich geometry using a diffuse reflector. In addition, it suggests than an increase in reflector surface area of an optically closed system, in an otherwise equivalent optical transport geometry, yields worse light capture efficiency properties. Furthermore, it is suggested that in some types of complex geometries, metallized reflectors can yield better light capture efficiency properties over diffuse reflectors; as well as suggesting the inverse for simple reflector geometries.

Future work may involve a comparison of Monte-Carlo obtained light capture efficiency results to actual experimental data on signal to noise ratio and resolution. In addition, detector virtualization is being considered. Detector virtualization is intended to utilize all applicable forms of Monte-Carlo particle transport combines with the simultaneous simulation of numerous real world physics processes inherent in the operation of a radiation detection system. The ultimate goal of detector virtualization will be to duplicate real-world detector response in a computer simulation, leading to the advancement of radiation detector sciences in the areas of understanding and development.

References

1. M.W. Cooper, J.I. McIntyre, T.W. Bowyer, A.J. Carman, J.C. Hayes, T.R. Heimbigner, C.W. Hubbard, L.S. Lidey, K.E. Litke, S.J. Morris, M.D. Ripplinger, R Suarez, and RC Thompson. *Redesigned Beta-Gamma Radioxenon Detector*. Nuclear Instruments and Methods in Physics Research. Section A, Accelerators, Spectrometers, Detectors and Associated Equipment 579(1):426-430 (2007).

2. Preparatory Commission for Comprehensive Nuclear-Test-Ban-Treaty Organization, *Operational Manual for Radionuclide and the International Exchange of Radionuclide Data*, CTBT/WGB/TL-11/5/Rev. 4 (1999).

3. G. F. Knoll, T. F. Knoll, T. M. Henderson. *Light Collection in Scintillation Detector Composites for Neutron Detection. University of Michigan and KMS Fusion Incorporated.* IEEE Transactions on Nuclear Science, Vol. 35, No. 1 (1988).

4. F. Cayouette, et al. *DETECT2000 User Manual.* Laval University, Canada (2001).

5. A. T. Farsoni, D. M. Hamby, K. D. Ropon, S. E. Jones. *A Two-Channel Phoswich Detector for Dual and Triple Coincidence Measurements of Radioxenon Isotopes.* Oregon State University (2007).

6. W. Henning, H. Tan, A. Fallu-Labruyere, W. K. Warburton, J. I. McIntyre, A. Gleyzer. *Design of a Phoswich Well Detector for Radioxenon Monitoring*. XIA, LLC, Pacific Northwest National Laboratory, PhotoPeak Inc. 28th Seismic Research Review: Ground-Based Nuclear Explosion Monitoring Technologies (2006).